

**SYNTHETIC PEPTIDE F2A4-K-NS MIMICS FGF-2  
IN VITRO AND IS ANGIOGENIC IN VIVO\***

**X. Lin<sup>1</sup>, K. Takahashi<sup>2</sup>, S.L. Campion<sup>2</sup>, Y. Liu<sup>2</sup>, G.G. Gustavsen<sup>3</sup>, L.A. Peña<sup>1,3</sup>, & P.O. Zamora<sup>2</sup>**

**From the <sup>1</sup>Medical Department, Brookhaven National Laboratory, Upton, NY; <sup>2</sup>BioSurface Engineering Technologies, Inc., College Park, MD; and the <sup>3</sup>Program in Biomedical Engineering, State University of New York, Stony Brook, NY**

Running title: Angiogenesis with an FGF-2 mimetic

Address correspondence to: X. Lin, BioSurface Engineering Technologies, Inc., 387 Technology Drive, College Park, MD 20742-3371, Tel: (301) 405-2193, Fax: (301) 314-2389; E-mail: xlin@biosetinc.com

**A multi-domain synthetic peptide, F2A4-K-NS, mimicked the action of recombinant human FGF-2 (rhFGF-2) *in vitro* and in an *in vivo* model of angiogenesis. Like rhFGF-2, F2A4-K-NS was quantitatively shown to bind to FGF receptors in a cell-free receptor binding assay using a chimeric FGFR1 (IIIc)/Fc and monitored by surface plasmon resonance (SPR), and also shown to bind to heparin using biotinylated low molecular weight heparin in a similar SPR assay. *In vitro*, F2A4-K-NS triggered signal transduction as monitored by the stimulation of ERK1/2 phosphorylation in human umbilical cord endothelial cells. In cell based assays, it increased cell migration, cell proliferation, and gelatinase secretion; endpoints associated with FGF-2 stimulation. Furthermore, these *in vitro* effects were mediated with quantities of F2A4-K-NS that were similar to that of rhFGF-2. *In vivo*, F2A4-K-NS was angiogenic at doses of 40- and 400 ng/implant in a subcutaneous implant assay as determined by morphologic scoring, hemoglobin content, and histology. These results support the hypothesis that F2A4-K-NS is a mimetic of FGF-2 that can substitute for FGF-2 *in vitro* and *in vivo*. A synthetic mimetic of FGF-2, such as F2A4-K-NS, could be a useful tool in studying mechanisms of cell activation and potentially in various therapeutic applications.**

## INTRODUCTION

A synthetic peptide that could mimic aspects of the bioactivity of recombinant human FGF-2 (rhFGF-2) could be of considerable interest, especially if one of those actions included stimulation of angiogenesis. While FGF-2 affects many cell types in a multiplicity of ways, its effect on angiogenesis (1, 2) underlies, at least in part, many of the therapeutic approaches for its use (3). Such potential uses include the treatment of ischemic heart and peripheral vascular disease, myocardial infarction, and diabetic retinopathy (3). Other potential applications for FGF-2 include preparation of artificial organ implant sites (4, 5), aneurysm healing and treatment (6-8), the treatment of diabetic foot ulcers, and acceleration bone fracture healing (9-12).

For a peptide to mimic the biological effects of FGF-2, it would be expected to bind to FGF receptor type-1 (FGFR1) (2) and in particular the “c”-splice variants (13). Receptor binding should lead to signal transduction which, in turn, would lead to increases in cell proliferation, migration, and secretion of proteases. Each of those events would be expected to participate in angiogenesis *in vivo*. Clearly, the aforementioned actions could also participate in a range of other tissue and wound responses stimulated by FGF-2.

In the studies presented here, F2A4-K-NS, a multi-domain synthetic peptide was evaluated for its ability to mimic aspects of rhFGF-2 bioactivity including the ability to stimulate angiogenesis in an experimental model. The results support the hypotheses that F2A4-K-NS can mimic rhFGF-2 bioactivity.

## MATERIALS & METHODS

*Peptide Synthesis.* Peptides in milligram quantities were synthesized manually following standard Fmoc protocols using NovaSyn TGR resin (EMD BioSciences, La Jolla, CA). Fmoc-amino acids including aminohexanoic acid (Ahx) were obtained from Peptides International, Inc. (Lexington, KY).

F2A4-K-NS was synthesized as a branched peptide with the following sequence:

H-YRSRKYSSWYVALKRRK(H-YRSRKYSSWYVALKR)-Ahx-Ahx-Ahx-RKRLDRIAR-NH<sub>2</sub>. It was purified by RP-HPLC on a C18 column, using a linear gradient 0–60% acetonitrile/water (0.1% trifluoroacetic acid) run over 60 min at 1 ml/min flow rate (detection at 214 nm). The purified peptide generated a single uniform peak on analysis by RP-HPLC. Software associated with the HPLC (Shimadzu Scientific Instruments, Inc., Columbia, MD) was used to determine the % area under the peptide peak (Table 1). The molecular mass of F2A4-K-NS, as determined by MALDI-TOF mass spectrometry, was 5539, in agreement with the theoretical molecular weight of 5540 Daltons.

F2A4-K-NS contains of two copies of the receptor-targeted sequence YRSRKYSSWYVALKRR derived from native FGF-2 (residues from 106 to 120) (14, 15), and a heparin binding domain, RKRLDRIAR that conforms to the canonical XBBBXXBX heparin-binding motif (16). In addition, F2A4RTDS, with the receptor-targeted sequence YRSRKYSSWYVALKRR of F2A4-K-NS was synthesized. A control peptide designated HBD3 was also synthesized and had the following sequence: Ahx-Ahx-Ahx-RKRLDRIAR-NH<sub>2</sub>. This peptide contained the heparin binding domain but lacked the receptor binding sequences.

*Surface Plasmon Resonance (SPR) Analysis.* Real-time biomolecular interactions were analyzed with a BIAcore 2000 system (Biacore Inc., Piscataway, NJ). F2A4-K-NS was synthesized as described above, and rhFGF-2 was obtained from the NIH/NCI Preclinical Repository, Biological Resource Branch. Soluble FGF receptor, recombinant chimera of human FGFR1 $\alpha$ (IIIc)/Fc (R & D Systems, Minneapolis, MN), was immobilized on research grade CM5 chips (Biacore Inc., Piscataway, NJ). Hereafter, FGFR1 $\alpha$ (IIIc)/Fc is referred to as FGFR1. Following activation with EDC/NHS, successful immobilization of FGFR1 was achieved by injecting FGFR1 (10  $\mu$ g/ml in HBS-EP buffer (0.01 M HEPES, pH 7.4, 0.15 M NaCl, 3 mM EDTA, 0.005% Tween 20 (v/v)) onto the activated CM5 chip. To obtain kinetic data, different concentrations of analytes in HBS-EP buffer were injected over the sensor chip at a flow rate of 50  $\mu$ l/min. Peptide binding was measured in resonance units (RU). At the end of each sample injection (120 s) HBS-EP buffer was passed over the sensor surface to monitor the dissociation phase. Reference responses from blank flow cells were subtracted from FGFR1 flow cells for each analyte injection and the kinetic parameters for each interaction were determined by globally fitting the experimental data to a 1:1 interaction with BIAEVALUATION software (Biacore Inc., Piscataway, NJ). The association rate constant and the dissociation rate constant ( $k_a$  and  $k_d$ , respectively) for FGFR1 interaction with F2A4RTDS can not be obtained by 1:1 Langmuir binding model, thus, the equilibrium dissociation constant ( $K_D$ ) was derived by a steady state binding model. A minimum of six different analyte concentrations were used to determine the kinetic parameters for each interaction. For each fitting, the standard error (SE) values for the association and dissociation rate were 1-2 orders of magnitude smaller than the respective association and dissociation constant values; and the Chi square was less than 10% of the Rmax in all case.

Alternatively, heparin was immobilized on a chip as described by Sheehan et al (17). Briefly, a low-molecular weight heparin (LMWH) surface was created by linking biotin-bound LMWH (Celsus, Inc., Cincinnati, OH) to a Biacore Streptavidin chip using injection buffer (0.3 M NaCl, 20 mM HEPES (pH 7.4), and 0.05% Tween 20) at 10 $\mu$ l/min for 2 minutes. Analytes were injected at a concentration series from 800 nM to 50 nM with running buffer (0.15 M NaCl, 2 mM CaCl<sub>2</sub>, 20 mM HEPES (pH 7.4), and 0.05% Tween 20) at 50  $\mu$ l/min for 2 minutes. At the end of injections, running buffer was passed over the sensor surface for 2 minutes to monitor the dissociation. Then, the sensor surface was regenerated by injection of regeneration buffer (2 M NaCl, 20 mM HEPES (pH 7.4), and 0.05% Tween 20) at 30 $\mu$ l/min for 2 minutes. Peptide binding was analyzed as above.

*Cell Culture.* HUVECs (Cambrex, East Rutherford, NJ) were grown in Endothelial Cell Medium-2 (EGM<sup>®</sup>-2, Cambrex, East Rutherford, NJ), supplemented with 5% FBS, and EGM-2 MV singlequots supplements (Cambrex), in a 37°C incubator with a humidified atmosphere containing 5% CO<sub>2</sub>. C3H10T<sup>1/2</sup> murine multi-potent stem cells were obtained from the American Type Culture Collection (Manassas, VA) and were grown in DMEM:F12 medium containing 15% newborn calf serum and antibiotics. Rat microvascular endothelial cells (RMEC) transformed by SV40 Large T-antigen (18, 19) were a gift from M. Goligorsky, Division of Nephrology and Hypertension, State University of New York at Stony Brook.

*Phosphorylation of ERK1/2.* HUVECs were stimulated with rhFGF-2 and F2A4-K-NS at the concentrations indicated in the figures in medium containing 1% newborn calf serum. After incubation for selected times, cells were lysed and processed for Western blot analysis on Hybond nitrocellulose membranes (Amersham Biosciences, Piscataway, NJ). The total and

phosphorylated ERK1/2 were revealed by antibodies recognizing total ERK1/2 (Sigma Aldrich, St. Louis, MO) and phosphorylated (Thr202 and Tyr204) (Cell Signaling, Beverly, MA) ERK1/2.

*Cell Proliferation.* Cell proliferation was monitored using a commercially available kit (MTS) (Promega, Madison, WI) based on a tetrazolium compound (3-(4,5-dimethylthiazol-2-yl)-5-(3-carboxymethoxyphenyl)-2-(4-sulfophenyl)-2H-tetrazolium, inner salt (MTS). Aliquots of  $1 \times 10^3$  RMEC cells were seeded into wells of 96-well plates and allowed to attach. The medium was replaced with one containing 1% new born calf serum plus F2A4-K-NS. After 3 days in culture, the relative cell number was monitored using MTS following the directions of the manufacturer.

*Migration Assays.* HUVECs and C3H10T $\frac{1}{2}$  cells were used as target cells and two different methods were used in the analysis, migration across a wound margin and migration through a coated membrane (20). For studies involving migration across a simulated wound margin, the cells were grown *in vitro* and used when approximately 90% confluent. A simulated wound was made by scrapping the cells away from the substrate. The cultures were rinsed and then incubated in DMEM: F12 medium containing 2% newborn calf serum with or without peptide (50 ng/ml). rhFGF-2 (50 ng/ml) was used as a positive control reference material. The cells were allowed to migrate for 6 hours after which the cells were fixed in buffered formalin. Migration was monitored via phase contrast microscopy. Cells that had migrated across the simulated wound margin were counted. At least five fields were counted for each data point. For studies involving migration through a coated membrane, the bottoms of Trans-well inserts (3  $\mu$ m pore size) were coated with a solution of growth factor reduced Matrigel® (BD Biosciences, San Jose, CA) and allowed to dry. Target cells were then placed in the upper chamber and the inserts placed into wells with medium containing rhFGF-2 or F2A4-K-NS. The cultures were maintained for 18 hours after which the cells on the membrane were fixed in buffered formalin. The cells on the lower side of the insert were then stained with bis-benzamide and the cells quantitated using fluorescence microscopy.

*Gelatinase Assay.* The RMECs were seeded at  $1.2 \times 10^5$  /ml in 24-well plates and allowed to attach overnight. The medium was replaced with serum-free DMEM containing peptides. After 48 hours, the medium (supernatant) was harvested and the gelatinase activity was measured with the MMP Gelatinase Activity Assay Kit (ECM700) from Chemicon (Temecula, CA). The CHEMICON MMP Gelatinase Activity Assay Kit utilizes a biotinylated gelatinase substrate, which is cleaved by active gelatinases (MMP-2 and MMP-9). Remaining biotinylated fragments are then added to a biotin-binding 96-well plate and detected with streptavidin-Enzyme complex. Addition of enzyme substrate results in a colored product, detectable by its optical density at 450nm. The optical density was inversely related to the amount of gelatinase in the sample.

*In Vivo Angiogenesis Assay.* The angiogenesis model was based on the use of Matrigel implants in C57BL/6 mice (21) The experiments were performed under an approved IACUC protocol in accordance with the United States Department of Agriculture, Department of Health and Human Services, and the NIH policies regarding the humane care and use of laboratory animals.

Animals were randomly assigned to each treatment group. Seven implant sites were used per treatment group. Growth factor reduced-Matrigel at 4°C (liquid state) was mixed with 0.1 or

1.0  $\mu\text{g/ml}$  of rhFGF-2 or F2A4-K-NS. Aliquots of 0.4 ml of Matrigel were injected subcutaneously in the mouse dorsal surface at the paraspinal space. The Matrigel, needle and syringe were kept on ice until the time of injection to prevent gelling in the needle. After 5 days the animals were euthanized and the Matrigel plugs were dissected away from the host tissue, photographed, and then frozen in sealed tubes and weighed. Two observers reviewed the photographs and rated the angiogenic response in double-blind fashion. The angiogenic score was rated on a scale of 0-3 as described by Lucidarme *et al.* (22). Plugs with no blood vessels were assigned a score of 0, those with few tiny peripheral vessels were assigned 1, and those with larger vessels with shallow penetration scored 2, and those with several large vessels with deep penetration were scored 3.

For an additional measure of vascularization, total hemoglobin levels in the Matrigel plugs were determined using aqueous extracts as described elsewhere (22). A 60  $\mu\text{l}$  aliquot of the extract was removed for analysis, in which hemoglobin was converted to hemoglobin-ferricyanate after a 5-minute incubation with 200  $\mu\text{l}$  of Drabkin's reagent (SigmaAldrich, St. Louis, MO) and quantified with a microplate reader at 525 nm using bovine hemoglobin as standard.

## RESULTS

SPR analysis was used to investigate the interaction between F2A4-K-NS and FGFR1, the predominant receptor for FGF-2. FGF-2 was used as a reference as SPR analysis of binding to FGFR1 has been described by others (25).

The intact F2A4-K-NS molecule, its receptor targeting domain, and its heparin-binding domain (HBD3) were each evaluated with FGFR1. F2A4-K-NS and its receptor targeting domain (F2A4RTDS) both bound to FGFR1, whereas the heparin binding domain (HBD3) did not (Table 2). Of interest, however, was the observation that F2A4-K-NS had an equilibrium dissociation constant ( $K_D$ ) lower than that of its receptor targeting domain (Table 2). The lower  $K_D$  of F2A4-K-NS most likely arises from the presence of two receptor targeting domains in each molecule. Nonetheless, the results indicate that the interaction of F2A4-K-NS with FGFR1 was mediated by the receptor-targeted domain, not the heparin binding domain.

When compared to FGF-2, F2A4-K-NS exhibited an association rate constant ( $K_a$ ) lower than that of FGF-2, indicative of a slower on-rate with FGFR 1 (Table 2). On the other hand, F2A4-K-NS also had dissociation rate constant ( $K_d$ ) lower than that of FGF-2, indicative of a slower off-rate. The estimated equilibrium dissociation constant ( $K_D$ ) for F2A4-K-NS was  $3.7 \times 10^{-7}$  M whereas that of FGF-2 was  $9.9 \times 10^{-8}$  M. The higher  $K_D$  of F2A4-K-NS may reflect the multiple receptor binding sites in FGF-2.

SPR assays were also used to establish that F2A4-K-NS could bind to heparin (Table 2). F2A4-K-NS had been synthesized to contain a heparin binding domain to mimic FGF-2 (and the FGF-receptor complex) (23, 24) which binds heparin a contributor to signal transduction. Relative to heparin, F2A4-K-NS had a higher  $K_a$ ,  $K_d$ , and  $K_D$  when compared to FGF-2.

As an aside, the  $K_D$  for the FGF-2/FGFR1 and FGF-2/heparin of 99 nM and 36 nM compare favorably with  $K_D$  values of 62 nM and 39 nM as reported by other investigators (25). Upon receptor binding and activation, FGF-2 induces a series signaling events including activate MAP kinase pathway. If F2A4-K-NS initiated signal transduction in a manner similar to

FGF-2, the MAP kinase pathway would be activated with consequent phosphorylation of ERK1/2 (pERK1/2). F2A4-K-NS increased pERK1/2 in HUVEC by 30 minutes after addition (Fig. 2). A similar extent of phosphorylation (pERK1/2) was found in cells stimulated with either 5 ng/ml or 50 ng/ml of F2A4-K-NS. FGF-2, which was used as a reference, increased pERK1/2 at 10 minutes, and thereafter the pERK1/2 returned to basal levels.

The consequence of signal transduction by F2A4-K-NS would be expected to be expression phenotypes typically associated with FGF-2 stimulation. Such changes could include increased cell proliferation and migration, protease secretion, and angiogenesis. In the endothelial cell line RMEC, a relative increase in cell number was found for all F2A4-K-NS concentration tested between 1- and 200 ng/ml (Fig. 3). C3H10T $\frac{1}{2}$  cells also increased proliferation in response to F2A4-K-NS (data not shown).

F2A4-K-NS treatment of cells also resulted increased *in vitro* migration of HUVECs across a simulated wound margin (Fig. 4a). To insure that migration was in fact stimulated, a different evaluation system, transwell migration, was used. In this system migration was also increased in HUVECs and C3H10T $\frac{1}{2}$  to levels averaging 136% and 170% of control values, respectively. FGF-2 increased migration by 119% and 116%, respectively for HUVEC and C3H10T $\frac{1}{2}$  cells. As FGF-2 can influence the production of gelatinases in a number of cell lines (26-28), F2A4-K-NS was evaluated for its ability to increase gelatinase activity. F2A4-K-NS treatment (5- and 50 ng/ml) of RMEC cells resulted in an increased secretion of gelatinase (Fig. 4b). rhFGF-2, which was used as a positive control, also increased the secretion of gelatinase.

Endothelial cell migration and gelatinase secretion are two key steps that association with angiogenesis *in vivo*. F2A4-K-NS induces cell migration and gelatinase secretion with similar efficacy as FGF-2, suggesting that it might also induce angiogenesis when introduced into animal. In this study we used an *in vivo* Matrigel plug assay to monitor the effects of F2A4-K-NS on angiogenesis, a hallmark of FGF-2. F2A4-K-NS stimulated angiogenesis (Fig. 5a), as did rhFGF-2, which was used as a system control. Angiogenic response as monitored by morphological scoring indicated a significant response to F2A4-K-NS at 40- and 400 ng/implant, a response that was verified by histological examination (data not shown). A quantitative assessment of the hemoglobin content of the plugs also indicated a significantly higher amount of hemoglobin in plugs that were implanted with F2A4-K-NS when compared to controls (Fig. 5b). The control peptide, HBD3 containing only the heparin binding domain (minus the receptor targeting domain) did not stimulate angiogenesis.

## DISCUSSION

The central hypothesis of this study was the peptide F2A4-K-NS could mimic aspects of FGF-2 bioactivity, and the results of this study support that contention. F2A4-K-NS is a multi-domain peptide with a branched design that incorporates two copies of an FGF receptor binding sequence from FGF-2, residues 106 to 120. Previous report shown that the linear version of this region, designated as FGF-(106-120) by Baird and colleagues, inhibits FGF-2 binding to FGF receptor on BHK cells and simulates thymidine incorporation in 3T3 cell when used in 500  $\mu$ g/ml, suggesting the linear peptide is a partial agonist (14). The FGF-(160-120) was also shown as a FGF-2 weak antagonist (15). In this study we shown that F2A4-K-NS, branched peptide construct with two receptor binding domains, possess 3 time higher affinity to FGFR1

than FGF-(106-120). Furthermore, F2A4-K-NS also possess FGF-2-like activity in similar dose range as recombinant FGF-2.

As a mimetic, F2A4-K-NS would be expected to exhibit similar, but not necessarily equivalent, binding to FGF receptors; and at least broadly result in the initiation of signal transduction, cell behavior, and phenotypes associated with FGF-2. The results from this study established that F2A4-K-NS bound to the receptor FGFR1 and also bound to heparin. It activated the receptor signaling cascade in cells as evidenced by increases in pERK1/2, and triggered a series of changes in cell behavior similar to that of induced by FGF-2. These changes included an increase in cell migration and cell proliferation, an increase in the secretion of gelatinase, and a stimulation of angiogenesis *in vivo*. Also, the quantities of F2A4-K-NS needed to illicit those effects were similar to that of rhFGF-2.

F2A4-K-NS bound to FGFR1 an affinity approximately one third that of rhFGF-2. Once bound, however, it had almost a 10 times slower dissociation rate from the receptor compared to FGF-2. The slower dissociation rate could arise from the juxtaposition of the dual receptor targeted sequences of F2A4-K-NS which would tend to reduce dissociation. A slow dissociation rate of F2A4-K-NS from the receptor might benefit overall receptor activation by kinetically favoring commitment of the receptor cytoplasmic domain to the active state.

Yet in spite of the slower dissociation rate, the net equilibrium binding constant of F2A4-K-NS to FGFR1 was lower than that of FGF-2. Nonetheless, the quantities of F2A4-K-NS needed to illicit biological effects were similar to that of rhFGF-2. This indicates that mechanisms in addition to receptor binding are likely involved in the bioactivity of F2A4-K-NS.

One factor that could contribute to the bioactivity of F2A4-K-NS is its ability to bind to heparin, and presumably heparan sulfate found on cell surfaces. In the current study, the equilibrium binding constant of F2A4-K-NS to heparin was approximately 2 times higher than that of FGF-2. F2A4-K-NS binding to heparin could mediate an increased biological effectiveness. This suggest a conceptually similarity to a signaling complex composed of heparin/FGF/FGFR as proposed by Ornitz (29). The signaling complex requires the assembly of a ternary complex of FGF, FGFR, and heparin (or heparan sulfate proteoglycan). Two models explain the association: the ternary complex can be formed by heparin binding two 1:1 FGF-FGFR complexes or heparin crosslinking two FGFs that in turn bring together two receptor chains (30). The binding of F2A4-K-NS to FGFR1 and also heparin would be conceptually permissive in either model.

The result of receptor dimerization, regardless of the exact mechanism, would lead to activation of the MAP kinase pathway and result in phosphorylation of ERK1/2. Treatment of cells with F2A4-K-NS resulted in an increase in ERK1/2. Interestingly, the phosphorylation of ERK1/2 induced by F2A4-K-NS appeared to take longer that of FGF-2: 30 minutes compared to 10 minutes. These observations may be consistent with the F2A4-K-NS/FGFR 1 binding kinetics with a slow rate association, but also a slow dissociation rate.

F2A4-K-NS treatment of cells also resulted in increased proliferation of endothelial cells and fibroblasts, increased cellular migration, and up-regulation of gelatinase secretion. While it is unlikely that F2A4-K-NS will be established to mimic each and every action of FGF-2, the changes in cell behavior observed in this study are consistent with known actions of FGF-2. Taken together with the other data presented here the observations support the contention that F2A4-K-NS mimics FGF-2.

Cell migration, cell proliferation, and protease secretion are processes, among others, involved in FGF-2 stimulated angiogenesis. Induction of angiogenesis is a well-known outcome associated with FGF-2 and is the centerpiece of many of the experimental therapies with rhFGF-2. F2A4-K-NS stimulated angiogenesis *in vivo* in a subcutaneous assay, as did FGF-2, again strengthening the contention that F2A4-K-NS mimics FGF-2.

In summary, we demonstrated that it is possible to produce a peptide, F2A4-K-NS, that mimics at least some of the actions of FGF-2 that is biologically active in quantities similar to the parental molecule, and that is active *in vivo*. The ability to construct synthetic molecules such as F2A4-K-NS allows for the systematic exploration of structure-function relationships, and consequent fine-tuning of the biological properties. Additionally, chemical synthesis is free of inherent biological contamination (nucleic acids, viruses, prion proteins, etc.) which may complicate purification of recombinant growth factors. Peptide synthesis uses readily available building blocks starting materials and is scalable. Also, it enables complete control over design and incorporation of non-coded elements which could improve biological activity.

## REFERENCES

1. Nugent, M. A. and Iozzo, R. V. Fibroblast growth factor-2. *Int J Biochem Cell Biol*, 32: 115-120, 2000.
2. Powers, C. J., McLeskey, S. W., and Wellstein, A. Fibroblast growth factors, their receptors and signaling. *Endocr Relat Cancer*, 7: 165-197, 2000.
3. Battegay, E. J. Angiogenesis: mechanistic insights, neovascular diseases, and therapeutic prospects. *J Mol Med*, 73: 333-346, 1995.
4. Sakurai, T., Satake, A., Sumi, S., Inoue, K., Nagata, N., Tabata, Y., and Miyakoshi, J. The efficient prevascularization induced by fibroblast growth factor 2 with a collagen-coated device improves the cell survival of a bioartificial pancreas. *Pancreas*, 28: e70-79, 2004.
5. Schnettler, R., Alt, V., Dingeldein, E., Pfefferle, H. J., Kilian, O., Meyer, C., Heiss, C., and Wensch, S. Bone ingrowth in bFGF-coated hydroxyapatite ceramic implants. *Biomaterials*, 24: 4603-4608, 2003.
6. van der Bas, J. M., Quax, P. H., van den Berg, A. C., Visser, M. J., van der Linden, E., and van Bockel, J. H. Ingrowth of aorta wall into stent grafts impregnated with basic fibroblast growth factor: a porcine *in vivo* study of blood vessel prosthesis healing. *J Vasc Surg*, 39: 850-858, 2004.
7. Hatano, T., Miyamoto, S., Kawakami, O., Yamada, K., Hashimoto, N., and Tabata, Y. Acceleration of aneurysm healing by controlled release of basic fibroblast growth factor with the use of polyethylene terephthalate fiber coils coated with gelatin hydrogel. *Neurosurgery*, 53: 393-400; discussion 400-391, 2003.
8. Matsumoto, H., Terada, T., Tsuura, M., Itakura, T., and Ogawa, A. Basic fibroblast growth factor released from a platinum coil with a polyvinyl alcohol core enhances cellular proliferation and vascular wall thickness: an *in vitro* and *in vivo* study. *Neurosurgery*, 53: 402-407; discussion 407-408, 2003.

9. Chen, W. J., Jingushi, S., Aoyama, I., Anzai, J., Hirata, G., Tamura, M., and Iwamoto, Y. Effects of FGF-2 on metaphyseal fracture repair in rabbit tibiae. *J Bone Miner Metab*, 22: 303-309, 2004.
10. Kawaguchi, H., Nakamura, K., Tabata, Y., Ikada, Y., Aoyama, I., Anzai, J., Nakamura, T., Hiyama, Y., and Tamura, M. Acceleration of fracture healing in nonhuman primates by fibroblast growth factor-2. *J Clin Endocrinol Metab*, 86: 875-880, 2001.
11. Nakamura, T., Hara, Y., Tagawa, M., Tamura, M., Yuge, T., Fukuda, H., and Nigi, H. Recombinant human basic fibroblast growth factor accelerates fracture healing by enhancing callus remodeling in experimental dog tibial fracture. *J Bone Miner Res*, 13: 942-949, 1998.
12. Radomsky, M. L., Thompson, A. Y., Spiro, R. C., and Poser, J. W. Potential role of fibroblast growth factor in enhancement of fracture healing. *Clin Orthop* S283-293, 1998.
13. Ornitz, D. M., Xu, J., Colvin, J. S., McEwen, D. G., MacArthur, C. A., Coulier, F., Gao, G., and Goldfarb, M. Receptor specificity of the fibroblast growth factor family. *J Biol Chem*, 271: 15292-15297, 1996.
14. Baird, A., Schubert, D., Ling, N., and Guillemin, R. Receptor- and heparin-binding domains of basic fibroblast growth factor. *Proc Natl Acad Sci U S A*, 85: 2324-2328, 1988.
15. Ray, J., Baird, A., and Gage, F. H. A 10-amino acid sequence of fibroblast growth factor 2 is sufficient for its mitogenic activity on neural progenitor cells. *Proc Natl Acad Sci U S A*, 94: 7047-7052, 1997.
16. Verrecchio, A., Germann, M. W., Schick, B. P., Kung, B., Twardowski, T., and San Antonio, J. D. Design of peptides with high affinities for heparin and endothelial cell proteoglycans. *J Biol Chem*, 275: 7701-7707, 2000.
17. Sheehan, J. P., Kobbervig, C. E., and Kirkpatrick, H. M. Heparin inhibits the intrinsic tenase complex by interacting with an exosite on factor IXa. *Biochemistry*, 42: 11316-11325, 2003.
18. Tsukahara, H., Gordienko, D. V., Tonshoff, B., Gelato, M. C., and Goligorsky, M. S. Direct demonstration of insulin-like growth factor-I-induced nitric oxide production by endothelial cells. *Kidney Int*, 45: 598-604, 1994.
19. Tsukahara, H., Ende, H., Magazine, H. I., Bahou, W. F., and Goligorsky, M. S. Molecular and functional characterization of the non-isopeptide-selective ETB receptor in endothelial cells. Receptor coupling to nitric oxide synthase. *J Biol Chem*, 269: 21778-21785, 1994.
20. Lee, M. S., Moon, E. J., Lee, S. W., Kim, M. S., Kim, K. W., and Kim, Y. J. Angiogenic activity of pyruvic acid in in vivo and in vitro angiogenesis models. *Cancer Res*, 61: 3290-3293, 2001.
21. Passaniti, A., Taylor, R. M., Pili, R., Guo, Y., Long, P. V., Haney, J. A., Pauly, R. R., Grant, D. S., and Martin, G. R. A simple, quantitative method for assessing angiogenesis and antiangiogenic agents using reconstituted basement membrane, heparin, and fibroblast growth factor. *Lab Invest*, 67: 519-528, 1992.
22. Lucidarme, O., Nguyen, T., Kono, Y., Corbeil, J., Choi, S. H., Varner, J., and Mattrey, R. F. Angiogenesis model for ultrasound contrast research: exploratory study. *Acad Radiol*, 11: 4-12, 2004.

23. Pellegrini, L., Burke, D. F., von Delft, F., Mulloy, B., and Blundell, T. L. Crystal structure of fibroblast growth factor receptor ectodomain bound to ligand and heparin. *Nature*, *407*: 1029-1034, 2000.
24. Ibrahimi, O. A., Yeh, B. K., Eliseenkova, A. V., Zhang, F., Olsen, S. K., Igarashi, M., Aaronson, S. A., Linhardt, R. J., and Mohammadi, M. Analysis of mutations in fibroblast growth factor (FGF) and a pathogenic mutation in FGF receptor (FGFR) provides direct evidence for the symmetric two-end model for FGFR dimerization. *Mol Cell Biol*, *25*: 671-684, 2005.
25. Ibrahimi, O. A., Zhang, F., Hrstka, S. C., Mohammadi, M., and Linhardt, R. J. Kinetic model for FGF, FGFR, and proteoglycan signal transduction complex assembly. *Biochemistry*, *43*: 4724-4730, 2004.
26. Allen, D. L., Teitelbaum, D. H., and Kurachi, K. Growth factor stimulation of matrix metalloproteinase expression and myoblast migration and invasion in vitro. *Am J Physiol Cell Physiol*, *284*: C805-815, 2003.
27. Weston, C. A. and Weeks, B. S. bFGF stimulates U937 cell adhesion to fibronectin and secretion of gelatinase B. *Biochem Biophys Res Commun*, *228*: 318-323, 1996.
28. Murphy, A. N., Unsworth, E. J., and Stetler-Stevenson, W. G. Tissue inhibitor of metalloproteinases-2 inhibits bFGF-induced human microvascular endothelial cell proliferation. *J Cell Physiol*, *157*: 351-358, 1993.
29. Ornitz, D. M. FGFs, heparan sulfate and FGFRs: complex interactions essential for development. *Bioessays*, *22*: 108-112, 2000.
30. Pellegrini, L. Role of heparan sulfate in fibroblast growth factor signalling: a structural view. *Curr Opin Struct Biol*, *11*: 629-634, 2001.

## FOOTNOTES

\* This research was supported in part by the U.S. Department of Energy (KP-1401020/MO-079, to L.A.P.). The BIAcore 2000 was used in cooperation with Proteomics Center core facility at the School of Medicine, State University of New York at Stony Brook.

<sup>1</sup> The abbreviations used are: FGF, fibroblast growth factor; SPR, surface plasmon resonance; ERK, extracellular signal-regulated kinase; HUVEC, human umbilical cord endothelial cell; HPLC, high performance liquid chromatography; MALDI-TOF, matrix assisted laser desorption/ionization- time of flight; LMWH, low-molecular weight heparin; HEPES, 4-(2-Hydroxyethyl)piperazine-1-ethanesulfonic acid; RMEC, rat microvascular endothelial cell; MAP, mitogen-activated protein.

## TABLE LEGENDS

Table 1. Chemical parameters associated with synthesis of F2A4-K-NS.

Table 2. F2A4-K-NS binding to FGFR 1 and heparin. The binding coefficient  $K_a$ ,  $K_d$ , and  $K_D$  values were determined by surface plasmon resonance binding assays of test compounds to immobilized FGFR-1IIIc/Fc or low-molecular weight heparin as described in the Methods section. N.B.; no binding. Chi square was less than 10% of Rmax in all cases.

## FIGURE LEGENDS

Fig. 1. Sensorgrams of F2A4-K-NS binding to FGFR 1. Surface plasmon resonance sensorgrams depict the interactions of F2A4-K-NS (A), FGF-2 (B), and with the FGFR-1IIIc/Fc chimera. For A & B, the analyte concentrations were 800, 400, 200, 100, 50, 25 nM. Sensorgrams depict the interaction of F2A4-K-NS (C) and FGF-2 (D) with biotinylated low molecular weight heparin. For C & D, the analyte concentrations were 400, 200, 100, 50, 25 nM. The kinetic and affinity constants calculated from this data are shown in Table 2.

Fig. 2. F2A4-K-NS induces MAP kinase ERK1/2 phosphorylation in HUVEC cells. HUVEC cells were treated with control peptide HBD3, FGF-2 or F2A4-K-N. After 10- or 30 minutes the cells were lysed, and equal amounts of cellular proteins were fractionated by SDS-PAGE and

transferred onto nitrocellulose. The Western blot was then probed with antibodies recognizing phosphorylated (Thr202 and Tyr204) ERK1/2 (upper panel) and total ERK1/2 (bottom panel).

Fig. 3. Effect of F2A4-K-NS on cell proliferation. REMC cells were seeded at 1000 cells per well of a 96-well plate and allowed to attach. The medium was changed to one containing low serum plus F2A4-K-NS and the cells incubated for 3 days after which MTS was added. Data is reported as the average  $\pm$  SD. Asterisks indicate  $p < 0.05$  determined by ANOVA followed by Bonferroni post hoc multiple comparisons versus the control group.

Fig. 4. Phenotypic behavior of synthetic peptide F2A4-K-NS compared to recombinant FGF-2. (A.) *Migration of HUVECs across a simulated wound margin in vitro.* HUVECs were grown to near confluency *in vitro*. A simulated wound was made by scrapping cells away from the substrate and after 6 hrs migration into the gap was monitored via microscopy. (B.) *Induction of gelatinase activity in RMECs in vitro.* RMECs were treated with vehicle or test compounds and after 48 hours the medium was collected and gelatinase activity determined as described in the Methods. Control vehicle, open bar  $\square$ ; FGF-2, hatched bar  $\square$ ; F2A4-K-NS, solid bar  $\blacksquare$ . For *Panels A, B*, data is reported as the average  $\pm$  SD. Asterisks indicate  $p < 0.05$  as determined by ANOVA followed by Bonferroni post hoc multiple comparisons versus the control group.

Fig. 5. Angiogenesis of F2A4-K-NS in subcutaneous Matrigel implants. Control vehicle, open bar  $\square$ ; FGF-2, hatched bar  $\square$ ; F2A4-K-NS, solid bar  $\blacksquare$ . (A.) *Morphologic score of angiogenesis.* Growth factor reduced Matrigel containing saline or test compounds was injected subcutaneously in mice and dissected out 5 days later. The gel plugs were scored on a scale of 0-3 as described in the Methods section with 0 indicating no blood vessels. (B.) *Hemoglobin content of subcutaneous Matrigel implants in mice.* The total hemoglobin (Hb) content of the implants was used as a quantitative index of angiogenesis. Hb was extracted from the plugs and detected colorimetrically. In all panels data is reported as the average  $\pm$  S.D. For *Panel C*, asterisks indicate  $p < 0.01$  as determined by the Mann-Whitney Rank Sum test. For *Panels D* asterisks indicate  $p < 0.05$  as determined by ANOVA followed by Bonferroni post hoc multiple comparisons versus the control group.

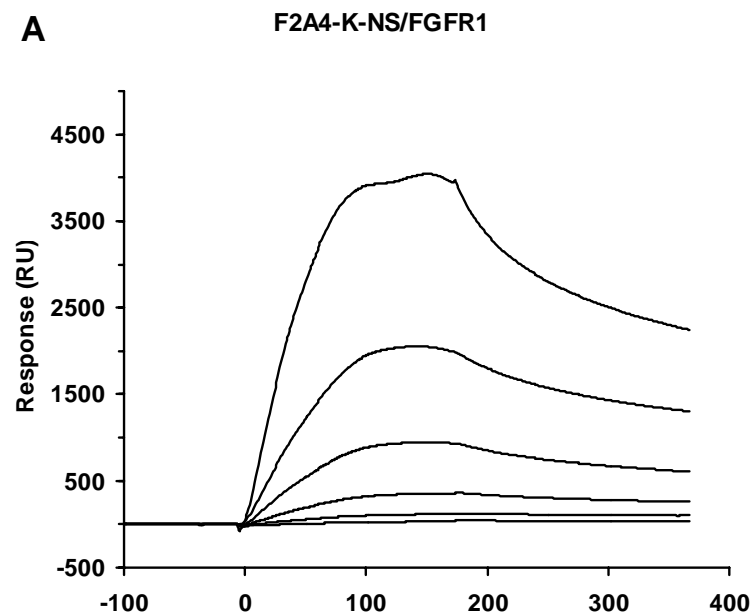
Table 1.

Yield from synthesis	Area under peptide peak	Molecular weight actual/predicted	mg peptide/mg lyophilized material
14%	>99%	5538/5540	0.7

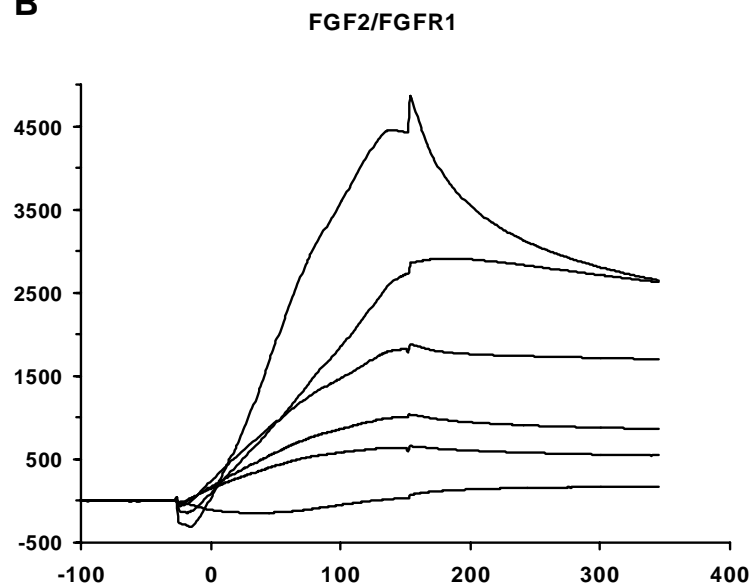
Table 2.

	Binding Coefficients		
	$K_a(M^{-1}s^{-1}) \times 10^3$	$K_d(s^{-1}) \times 10^{-4}$	$K_D(M)$
<b>F2A4-K-NS / FGFR1</b>	$4.1 \pm 0.8$	$15.3 \pm 0.2$	$3.74 \times 10^{-7}$
<b>FGF-2 / FGFR1</b>	$108.0 \pm 1.3$	$107.0 \pm 2.7$	$9.9 \times 10^{-8}$
<b>F2A4RTDS / FGFR1</b>			$1.12 \times 10^{-6}$
<b>HBD3/FGFR1</b>			N.B.
<b>F2A4-K-NS / Heparin</b>	$17.4 \pm 0.4$	$12.9 \pm 0.5$	$7.4 \times 10^{-8}$
<b>FGF-2 / Heparin</b>	$7.3 \pm 0.2$	$2.6 \pm 0.2$	$3.6 \times 10^{-8}$

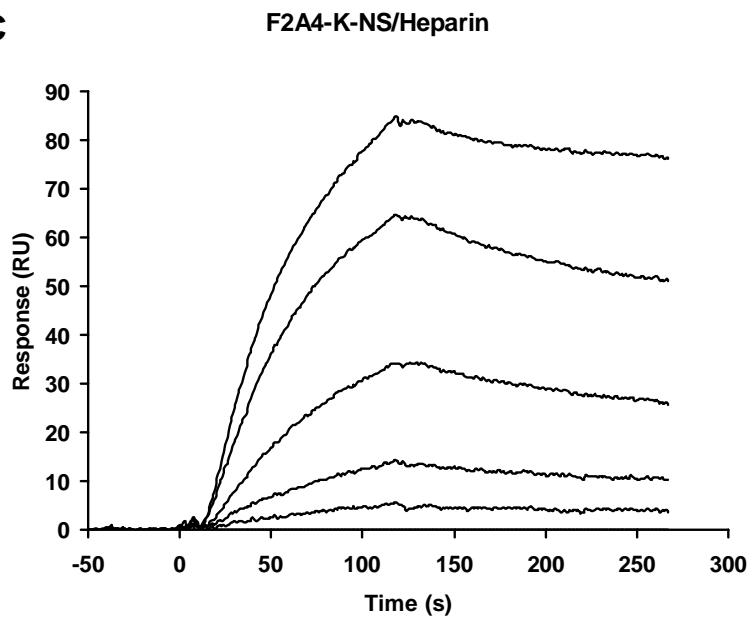
Figure 1. A



B



C



D

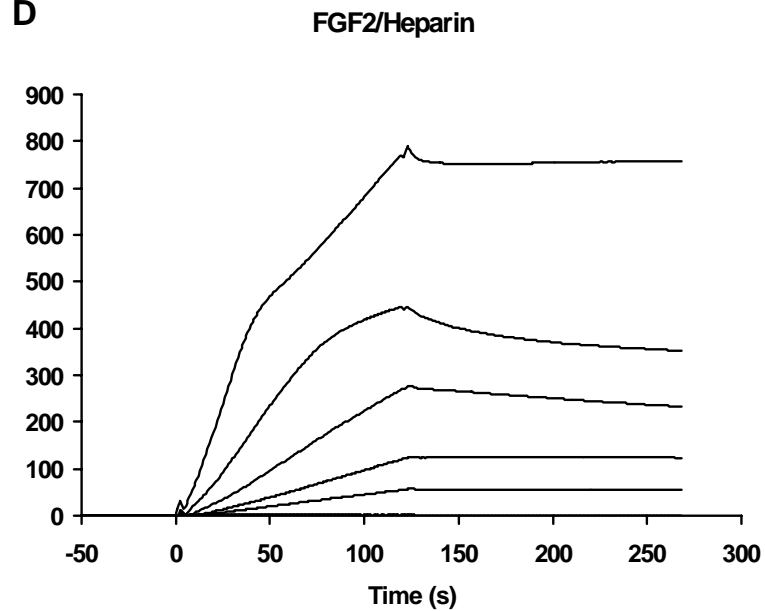


**Figure 2.**

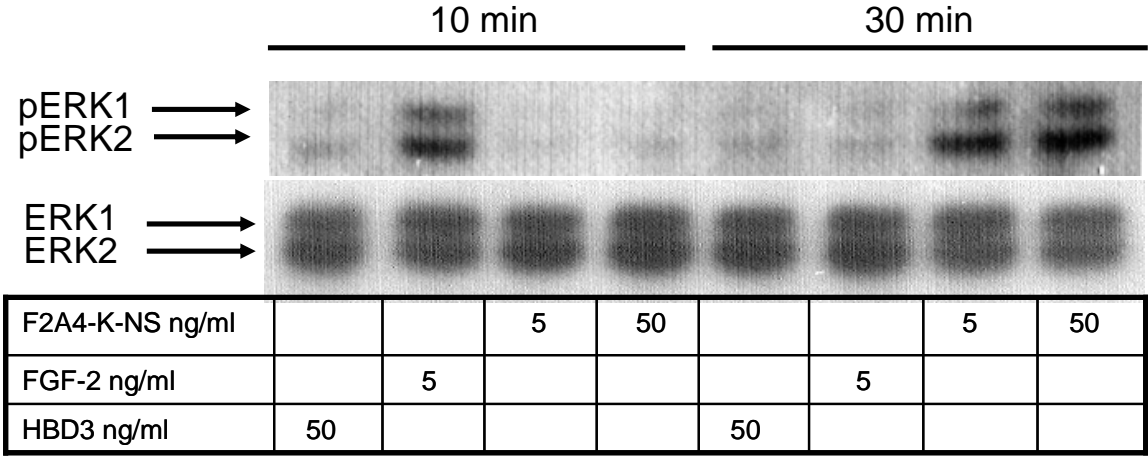
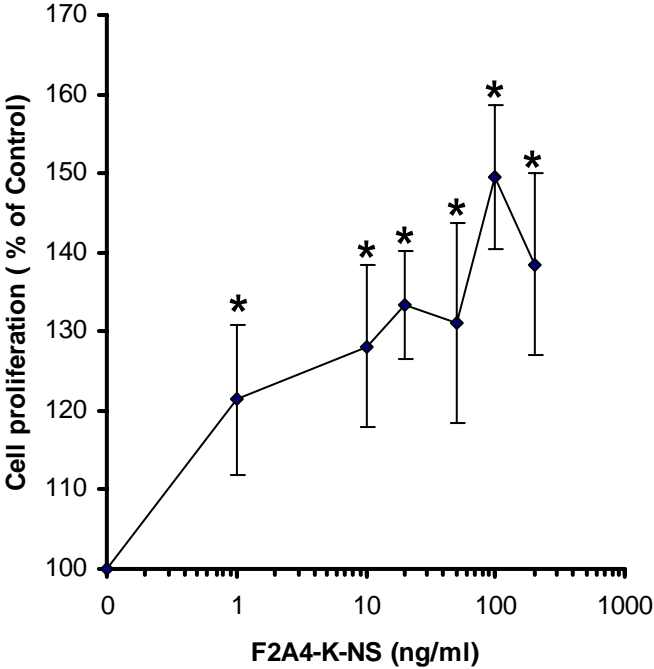


Figure 3.



**Figure 4.**

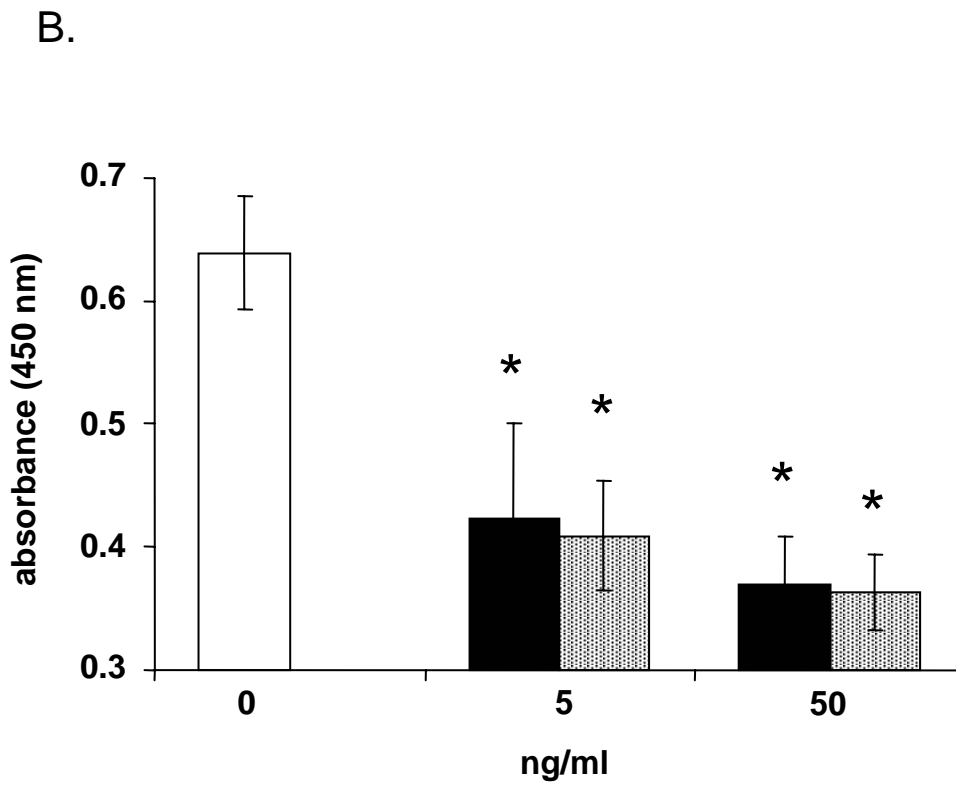
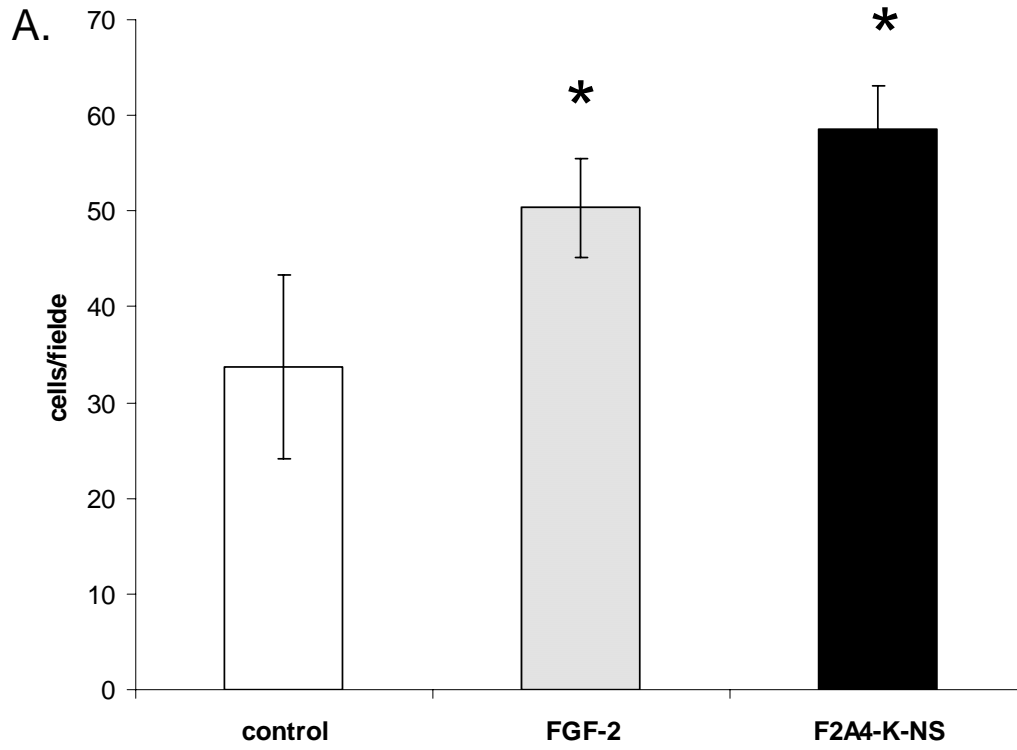


Figure 5.

